Journal of Biomolecular NMR, 8 (1996) 357–359
ESCOM

J-Bio NMR 395

A 3D NOESY-(HCACO)NH experiment for the measurement of NOEs involving $^1H^\alpha$ in ^{13}C-/^{15}N-labeled proteins dissolved in H_2O

Weixing Zhang and William H. Gmeiner*

The Eppley Institute for Research in Cancer and Allied Diseases, The University of Nebraska Medical Center, Omaha, NE 68198-6805, U.S.A.

Received 31 July 1996
Accepted 15 September 1996

Keywords: Pulsed-field gradient; NOE; Hck; SH2

Summary

A 3D NOESY-(HCACO)NH experiment is described that transfers NOEs from $^1H^\alpha$ to the backbone $^1H^N$ in the succeeding residue for detection. Using this strategy, NOEs involving $^1H^\alpha$ protons that resonate exactly at the water frequency can be detected. NOEs from an overlapping $^1H^\alpha$ proton that is attached to degenerate $^{13}C^\alpha$ can also be resolved. The performance of this approach is demonstrated for the ^{13}C-/^{15}N-labeled Hck/SH2 dissolved in H_2O.

Determination of NOEs for backbone protons is very important for NMR structural studies of proteins. Experiments for the determination of NOEs involving amide protons ($^1H^N$) require protein samples dissolved in H_2O (Marion et al., 1989a; Kay et al., 1990; Sklenář et al., 1993), while experiments for the detection of NOEs involving α-protons ($^1H^\alpha$) are normally performed on samples dissolved in D_2O (Ikura et al., 1990; Clore et al., 1991; Vuister et al., 1993). Conducting NMR experiments using separate isotopically enriched samples not only increases the cost of protein production, it also causes discrepancies in chemical shifts due to isotope effects and variation in sample conditions (Kay, 1993; Kay et al., 1993). Therefore, it is advantageous to record all NMR spectra necessary for the determination of a protein structure using a single H_2O sample. For this purpose, Muhandiram et al. (1993) have developed a ^{13}C-edited gd-NOESY-HSQC experiment for protein samples dissolved in H_2O. Although excellent water suppression was achieved using the gd-NOESY-HSQC experiment, signals from $^1H^\alpha$ protons that resonate exactly at the water frequency are very difficult to observe. Furthermore, some residues in proteins may have degenerate $^1H^\alpha$ and $^{13}C^\alpha$ chemical shifts, resulting in overlapped peaks in the NOESY-HSQC spectrum. Recently, we have demonstrated that overlapped NOEs from $^1H^N$ in a ^{15}N-edited NOESY-HSQC spectrum can be resolved using a $^{13}C'$-edited NOESY-H(N)CO experiment (Zhang et al., 1996). Here, we present a 3D NOESY-(HCACO)NH pulse sequence that transfers NOEs from $^1H^\alpha$ to the backbone $^1H^N$ in the succeeding residue for detection. The pulse scheme is illustrated in Fig. 1 and is briefly described below. The path of magnetization transfer can be described as:

$$^1H^{(i)}(t_1) \xrightarrow{NOE} {}^1H^{\alpha(j)} \xrightarrow{J_{C^\alpha H^\alpha}} {}^{13}C^{\alpha(j)} \xrightarrow{J_{C^\alpha C'}}$$

$$^{13}C'^{(j)} \xrightarrow{J_{CN}} {}^{15}N^{(j+1)}(t_2) \xrightarrow{J_{NH}} {}^1H^{N(j+1)}(t_3)$$

where the active couplings involved in each magnetization-transfer step are indicated above the arrows. Following the NOESY mixing period, $^1H^\alpha$ magnetization in residue j is transferred to $^1H^N$ in residue j + 1 using multiple INEPT-type transfer steps. The chemical shifts of $^1H^{(i)}$, $^{15}N^{(j+1)}$, and $^1H^{N(j+1)}$ evolve during t_1, t_2, and t_3, respectively. Pulsed-field gradient pulses are incorporated into the pulse sequence to aid the elimination of artifacts. Unwanted transverse magnetization and two-spin-order coherences that are present during the NOESY mixing period are destroyed by gradient pulses g1 and g2, respectively (Vuister et al., 1993). Artifacts due to imperfection

*To whom correspondence should be addressed.

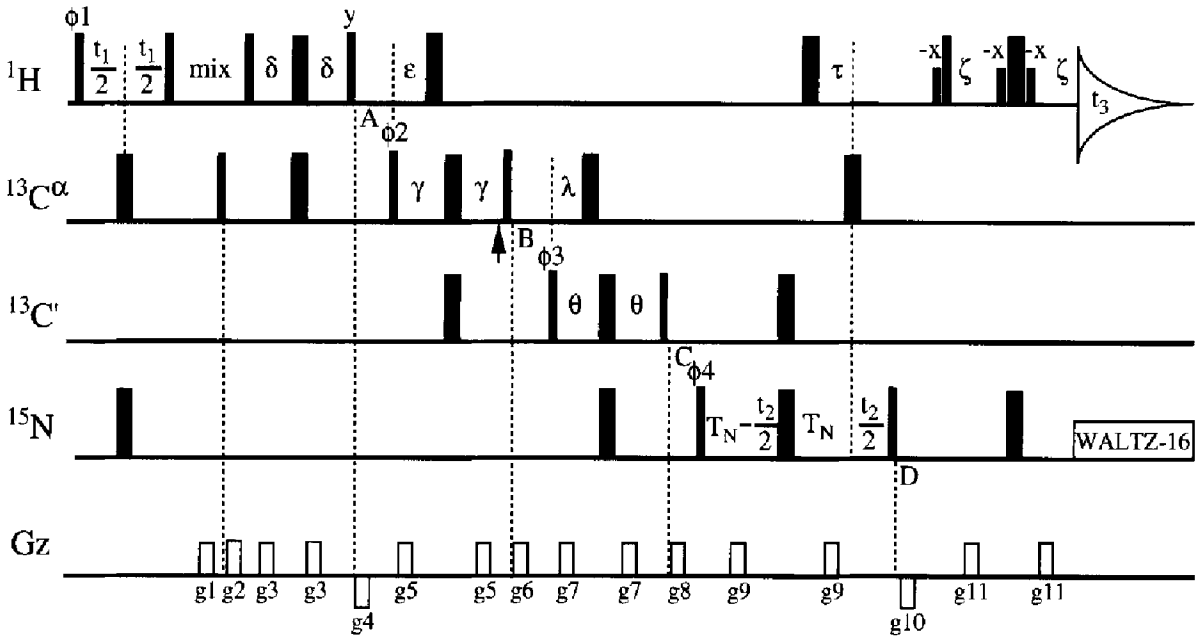

Fig. 1. Pulse scheme of the 3D NOESY-(HCACO)NH experiment. Narrow and wide pulses have flip angles of 90° and 180°, respectively. All pulses are applied along the x-axis, unless otherwise indicated. The letters A, B, C, and D indicate the position at which useful magnetization is in zz order. All ^{15}N pulses are applied at 117 ppm with an rf field strength of 6.25 kHz. The ^{13}C carrier was placed at 58 ppm at the beginning of the experiment and shifted to 175 ppm at point B. The rf field strength of the ^{13}C pulse from the beginning to point A is 16 kHz. The rf field strength for all ^{13}C' and ^{13}C$^{\alpha}$ 90° pulses following point B is 4.0 kHz, while for on-resonance ^{13}C' 180° and ^{13}C$^{\alpha}$ 180° pulses it is 9.0 kHz. The ^{13}C' 180° pulse between points A and B, and the ^{13}C$^{\alpha}$ 180° pulses between points B and C are applied as phase-modulated pulses (Patt, 1992) at an rf field strength of 4.0 kHz. The arrow indicates the position at which a 180° ^{13}C' pulse is applied to compensate for the Bloch–Siegert effect (Kay, 1993). The ^{1}H carrier is placed at the frequency of H_2O and the water-selective 90°-x pulse is applied at an rf field strength of 200 Hz. ^{15}N decoupling during acquisition is achieved using a WALTZ-16 scheme (Shaka et al., 1983) at an rf field strength of 1.0 kHz. The delay durations are $\delta = 1.6$ ms, $\varepsilon = 1.8$ ms, $\gamma = 3.3$ ms, $\lambda = 4.5$ ms, $\theta = 12.5$ ms, $\tau = 2.75$ ms, $\zeta = 2.4$ ms, and $T_N = 12.5$ ms. The durations and strengths of the pulsed-field gradient pulses are g1 = 3 ms, 12 G/cm, g2 = 2 ms, 10 G/cm, g3 = 0.5 ms, 8 G/cm, g4 = 0.5 ms, −15 G/cm, g5 = 0.5 ms, 10 G/cm, g6 = 0.5 ms, 15 G/cm, g7 = 0.8 ms, 12 G/cm, g8 = 0.5 ms, 16 G/cm, g9 = 0.2 ms, 10 G/cm, g10 = 0.5 ms, −18 G/cm, and g11 = 0.6 ms, 12 G/cm. All gradient pulses are rectangular and are applied along the z-axis. A delay of at least 200 μs is inserted between a gradient pulse and the subsequent rf pulse. The phase cycle is ϕ1 = x,−x; ϕ2 = 2x,2(−x); ϕ3 = 4x,4(−x); ϕ4 = 8x,8(−x); receiver = x,2(−x),x,−x,2x,2(−x),2x,−x,x,2(−x),x. Quadrature detection in t_1 and t_2 is achieved using the States–TPPI method (Marion et al., 1989b) by incrementing the phases of ϕ1 and ϕ4 independently.

of 180° pulses in the middle of each INEPT-type transfer step are removed by the gradient pulse pairs g3, g5, g7, g9, and g11, respectively (Kay, 1993; Kay et al., 1993). Gradient pulses g4, g6, g8, and g10 are used as zz filters to dephase undesired coherences (Wider and Wüthrich, 1993). The WATERGATE technique (Piotto et al., 1992) is employed to suppress the water signal for data acquisition. The water 90°-x selective pulse at point D is used to preserve the water magnetization that has returned to the z-axis during the experiment. Since several transfer steps are involved in this experiment, the absolute intensities of the NOE cross peaks also depend on some other factors unrelated to distance, such as relaxation times, coupling constants, and amide proton exchange rates. For a particular residue, however, cross-peak intensities are influenced by the same factors, allowing for the determination of interproton distances based on relative NOE intensities.

The performance of the 3D NOESY-(HCACO)NH experiment was tested using a ^{15}N-/^{13}C-labeled Hck/SH2 domain and the results are presented in Fig. 2. The protein sample (~ 3 mM) was dissolved in 90% H_2O/10% D_2O containing 100 mM NaCl, 5 mM DTT, and 50 mM sodium phosphate at pH 6.4. Data acquisition was performed at 30 °C using a Varian UNITY 500 NMR spectrometer equipped with a 5-mm triple-resonance PFG probe. Figure 2A shows NOEs from residues Asn^{25}, Met^{26}, Tyr^{49}, Val^{57}, and Tyr^{60}. The chemical shifts of ^{1}H$^{\alpha}$ in these residues are the same as that of H_2O and NOEs for these α-protons are difficult to observe using a ^{13}C-edited NOESY-HSQC experiment for samples dissolved in H_2O, but these NOEs are easily determined here. Figure 2B shows NOEs from ^{1}H$^{\alpha}$ in residues Lys^{39}, Asp^{86}, and Lys^{90}. The chemical shifts for both ^{1}H$^{\alpha}$ and ^{13}C$^{\alpha}$ are degenerate in these residues, giving overlapped peaks in a normal ^{13}C-edited NOESY-HSQC spectrum (data not shown). However, the chemical shifts of the ^{15}N and ^{1}H^N in the succeeding residues do not overlap, giving well-resolved NOE cross peaks in the NOESY-(HCACO)NH spectrum.

In summary, a 3D NOESY-(HCACO)NH experiment

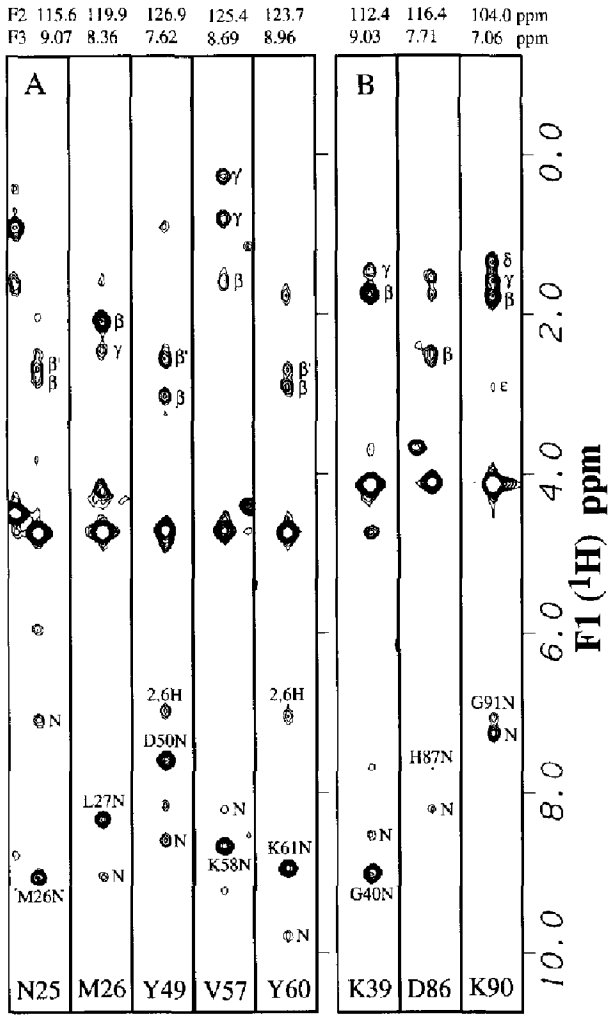

Fig. 2. F1 strips from the 3D NOESY-(HCACO)NH spectrum of Hck/SH2. (A) NOEs from $^1H^\alpha$ in residues Asn[25], Met[26], Tyr[49], Val[57], and Tyr[60]. The chemical shifts of the $^1H^\alpha$ protons in these residues are the same as that of the H_2O resonance. (B) NOEs from $^1H^\alpha$ in residues Lys[39], Asp[86], and Lys[90]. These residues have both degenerate $^1H^\alpha$ and degenerate $^{13}C^\alpha$ chemical shifts. The data were obtained from a $96(t_1) \times 32(t_2) \times 256(t_3)$ complex matrix with spectral widths of 6000, 1500 and 6000 Hz, respectively. A 16-step phase cycle and a relaxation delay of 0.8 s were used. The mixing period was 100 ms. After processing using FELIX (v. 2.05, Hare Research, Inc., Bothell, WA, U.S.A.), including linear prediction in the t_1 and t_2 time domains, the absorptive part of the final 3D spectrum comprised $256 \times 128 \times 256$ real points. Assigned intraresidue NOEs are labeled as N, α, β, β' etc., while interresidue NOEs are indicated with proper contacts.

has been presented for the determination of NOEs involving $^1H^\alpha$ in ^{13}C-/^{15}N-labeled proteins dissolved in H_2O. Using this technique, NOEs from $^1H^\alpha$ protons that resonate exactly at the H_2O frequency can be measured. Overlapping NOEs in the normal ^{13}C-edited NOESY-HSQC spectrum can also be resolved.

Acknowledgements

The authors acknowledge NMR instrumental assistance from David Babcook. This research was supported in part by the NIH-NCI CA-36727, the American Cancer Society (IRG-165G) and the Nebraska Department of Health.

References

Clore, G.M., Kay, L.E., Bax, A. and Gronenborn, A.M. (1991) *Biochemistry*, **30**, 12–18.

Ikura, M., Kay, L.E., Tschudin, R. and Bax, A. (1990) *J. Magn. Reson.*, **86**, 204–209.

Kay, L.E., Clore, G.M., Bax, A. and Gronenborn, A.M. (1990) *Science*, **249**, 411–414.

Kay, L.E. (1993) *J. Am. Chem. Soc.*, **115**, 2055–2057.

Kay, L.E., Xu, G.-Y., Singer, A.U., Muhandiram, D.R. and Forman-Kay, J.D. (1993) *J. Magn. Reson.*, **B101**, 333–337.

Marion, D., Kay, L.E., Sparks, S.W., Torchia, D.A. and Bax, A. (1989a) *J. Am. Chem. Soc.*, **111**, 1515–1517.

Marion, D., Ikura, M., Tschudin, R. and Bax, A. (1989b) *J. Magn. Reson.*, **85**, 393–399.

Muhandiram, D.R., Farrow, N.A., Xu, G.-Y., Smallcombe, S.H. and Kay, L.E. (1993) *J. Magn. Reson.*, **B102**, 317–321.

Patt, S.L. (1992) *J. Magn. Reson.*, **96**, 94–102.

Piotto, M., Saudek, V. and Sklenář, V. (1992) *J. Biomol. NMR*, **2**, 661–665.

Shaka, A.J., Keeler, J., Frenkiel, T. and Freeman, R. (1983) *J. Magn. Reson.*, **52**, 335–338.

Sklenář, V., Piotto, M., Leppik, R. and Saudek, V. (1993) *J. Magn. Reson.*, **A102**, 241–245.

Vuister, G.W., Clore, G.M., Gronenborn, A.M., Powers, R., Garrett, D.S., Tschudin, R. and Bax, A. (1993) *J. Magn. Reson.*, **B101**, 210–213.

Wider, G. and Wüthrich, K. (1993) *J. Magn. Reson.*, **B102**, 239–241.

Zhang, W., Smithgall, T.E. and Gmeiner, W.H. (1996) *J. Magn. Reson.*, **B111**, 305–309.